AN ANALYSIS OF THE ELECTROMAGNETIC FIELD IN A DOUBLE-POLAR LINEAR INDUCTION SYSTEM

Todorka Chervenkova

Technical University in Sofia , Faculty of Engineering and Pedagogy of Sliven
Department of Electrical Engineering
59 , Bourgasko shaussee Blvd., 8800 Sliven , BULGARIA
e-mail : tchervenkova@tu-sliven.bia-bg.com

Abstract

In this paper a new model for determination of the electromagnetic field components of linear induction system with a moving part is described. The analysis is done by four-dimensional electromagnetic potentials $\vec{\Psi}^{\varepsilon}$ *using the theory of the magnetic loops. A model of the variable magnetic charge defined by sufficiently thin solenoid without scattering with variable magnetic flux* $\Phi(t)$ *is also used. The vector components of the excited magnetic field* $\vec{H}$ *and the induced electric field* $\vec{E}$ *are determined in the Minkowski's space as elements of the dual Maxwell's tensor. The results obtained are compared with those got from the analysis made by the finite elements method.*

Keywords*: Linear induction system, four-dimensional electromagnetic potential, magnetic loops, Minkowski's space, Maxwell's tensor, finite elements methodh .*

1. INTRODUCTION

The determination of the electromagnetic field in linear induction system (LIS) at the presence of movement is considered.

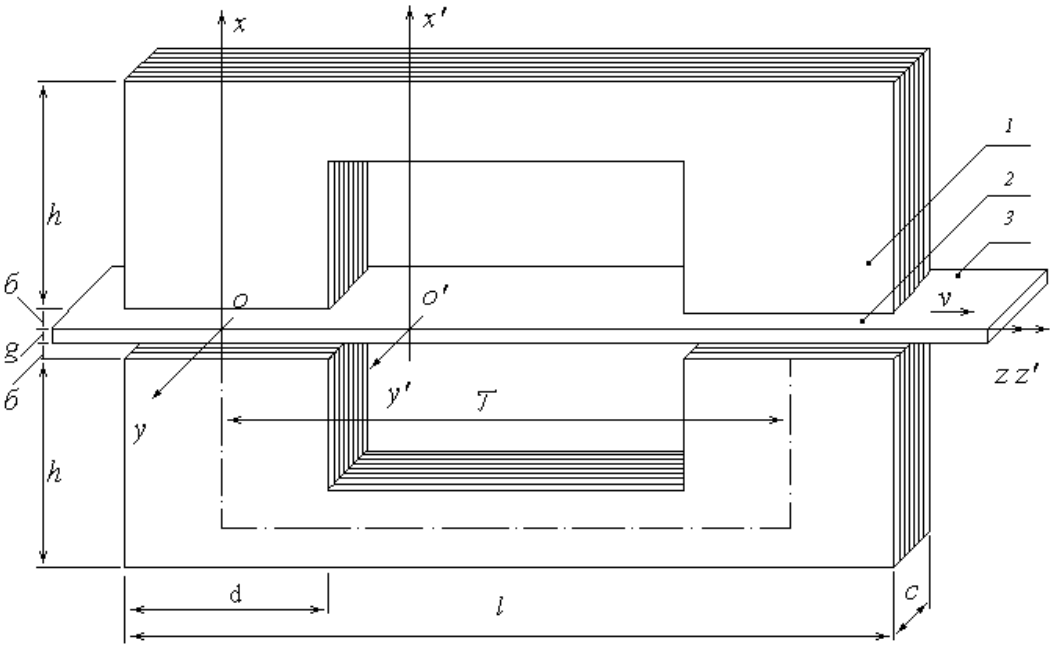

1- magnetic yoke, 2 –air gap, 3 –metal sheet ;

h , l – height and length of the inductor, respectively; *d* , *c*- length and width of the pole, respectively ;

б – air gap; *g* – thickness of the conductive sheet.

Figure 1. An idealized model of double-polar induction system

The LIS is power supplied by sinusoidal single-phase generator. The model of the LIS is represented in Fig.1. The magnetic system is symmetric because of the presence of a magnetic yoke with two inductors. The metal sheet placed in the air gap is moving with a constant velocity $v = const$ in the direction of one of the coordinate axes.

The magnetic loop is connected with the fixed XOYZ while the metal sheet with the mobile X'O'Y'Z' coordinate system.

A model of variable magnetic charge defined by sufficiently thin semi-endless solenoid without scattering with variable magnetic flux $\Phi(t)$ is used [1].

The cross-section S of the magnetic pole is considered to be consisted of n – number magnetic charges (in this case n =5). Fig. 2. represents the magnetic yoke composed of " n " – number magnetic loops.

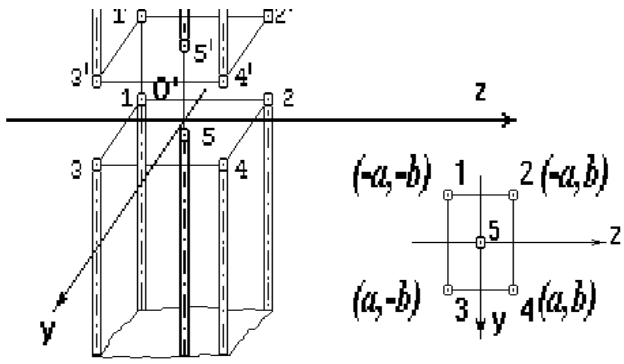

Figure 2. A model of the magnetic pole

c = 2a is the pole length , d = 2b is the pole width

The magnetic charge possesses variable sinusoidal magnetic flux

$$\Phi(t) = \Phi_m \sin(\omega t + \psi) \ , \tag{1}$$

where Φ_m is the amplitude of the magnetic flux , ω is the circular frequency and ψ is the initial phase.

2. RESULTS

2.1. ELECTROMAGNETIC POTENTIALS

The loop with a variable magnetic flux excites an electromagnetic field with electric vector-potential $\vec{A}_\varepsilon$ [2]

$$\vec{A}_\varepsilon = \frac{\varepsilon}{20\pi}\left\{\sum_{i=1}^{5}\sum_{k=1}^{2}\iiint_{(v)} \frac{\partial B/\partial t}{r}\, dv\right\} = \varepsilon\frac{e(t)}{20\pi}\left\{\sum_{i=1}^{5}\sum_{k=1}^{2}\int_{-l}^{-\delta}\frac{\vec{dl}}{r} + \sum_{i=1}^{5}\sum_{k=1}^{2}\int_{\delta}^{l}\frac{\vec{dl}}{r}\, dr\right\} \tag{2}$$

At an arbitrary point of the coordinate system XOYZ the scalar magnetic potential V_μ is the following

$$V_\mu = \sum_{i=1}^{5}\sum_{k=1}^{2}\int_{-\delta}^{\delta}\vec{H}d\vec{l} = \sum_{i=1}^{5}\sum_{k=1}^{2}\frac{\Phi}{20\pi\mu}\int_{-\delta}^{\delta}\frac{1}{r}dr \tag{3}$$

A four-dimensional electromagnetic potential $\vec{\Psi}_{(\varepsilon)}$ is introduced

$$\vec{\Psi}_{(\varepsilon)} = \{\Psi_{1\varepsilon}, \Psi_{2\varepsilon}\Psi_{3\varepsilon}\Psi_{4\varepsilon}\} = \left\{A_{\varepsilon x}, A_{\varepsilon y}A_{\varepsilon z}, \frac{j}{c}V_\mu\right\}, \tag{4}$$

where $A_{\varepsilon x}, A_{\varepsilon y}, A_{\varepsilon z}$ are the components of the vector-electric potential $\vec{A}_\varepsilon$ in the direction of the axes x, y, z and V_μ is the scalar magnetic potential.

The transformations of Lorentz [1, 2 , 5] for the electromagnetic potentials

$$A_{\varepsilon x} = A'_{\varepsilon x'}\ ;\ A'_{\varepsilon y} = A'_{\varepsilon y'}\ ;\ A'_{\varepsilon z} = \alpha\left(A'_{\varepsilon z'} + \frac{v}{c^2}V'_\mu\right);\ V_\mu = \alpha\left(V'_\mu + vA'_{\varepsilon z'}\right), \tag{5}$$

where :

$$\alpha = \frac{1}{\sqrt{1 - v^2/c^2}} \text{ is the relative factor; } c \text{ is the speed of light} \tag{6}$$

and the transformations of Lorentz concerning the coordinates

$$x' = x\ ,\ y' = y\ ,\ z' = \alpha(z - vt),\ t' = \alpha\left(t - \frac{v}{c^2}z\right) \tag{7}$$

in the Minkowski's space $\vec{X} = \{x, y, z, jct\}$ are used. At lower speed $v \langle\langle c\ (\alpha \approx 1)$ the transformations of Galiley are used

$$x' = x\ ,\ y' = y\ ,\ z' = (z - vt),\ t' = t\ . \tag{8}$$

It is supposed [2]

$$\Phi'(t') = \Phi(t),\ e(t) = -\frac{d\Phi}{dt} \approx \frac{d\Phi'(t')}{dt'}\ . \tag{9}$$

the condition $\Phi'(t') = \Phi(t)$ is introduced by analogy to the condition $J'(t') = J(t), i'(t') = i(t)$ [1, 2 , 4].

For the four-dimensional electromagnetic potential $\vec{\Psi}_{(\varepsilon)}$ is obtained

$$\vec{\Psi}_{\varepsilon} = \left\{ \begin{array}{c} A_{\varepsilon x} = \varepsilon \dfrac{e(t)}{4\pi} \dfrac{1}{5} \sum_{i=1}^{5} \sum_{k=1}^{2} \left(\begin{array}{c} Arsh \dfrac{x+\delta}{\sqrt{P_{ik}}} - Arsh \dfrac{x+h}{\sqrt{P_{ik}}} + \\ + Arsh \dfrac{x-h}{\sqrt{P_{ik}}} - Arsh \dfrac{x-\delta}{\sqrt{P_{ik}}} \end{array} \right) \\ A_{\varepsilon y} = 0 \\ A_{\varepsilon z} = \dfrac{\alpha \varepsilon v}{20\pi \mu c^2} \sum_{i=1}^{5} \sum_{k=1}^{2} \left(\dfrac{\Phi_k(t)}{\sqrt{Q_{ik}}} - \dfrac{\Phi_k(t)}{\sqrt{M_{ik}}} \right) \\ V_{\mu} = \dfrac{j}{c} \dfrac{\alpha}{20\pi \mu} \sum_{i=1}^{5} \sum_{k=1}^{2} \left(\dfrac{\Phi_k(t)}{\sqrt{Q_{ik}}} - \dfrac{\Phi_k(t)}{\sqrt{M_{ik}}} \right) \end{array} \right\} \tag{10}$$

where : $P_{ik} = (y + a_i)^2 + \{\alpha[(z + d_k) - vt] + b_i\}^2$;

$$Q_{ik} = (x+\delta)^2 + (y + a_i)^2 + \{\alpha[(z + d_k) - vt] + b_i\}^2$$

$$M_{ik} = (x-\delta)^2 + (y + a_i)^2 + \{\alpha[(z + d_k) - vt] + b_i\}^2$$

$$C_{ik} = (x+h)^2 + (y + a_i)^2 + \{\alpha[(z + d_k) - vt] + b_i\}^2$$

$$D_{ik} = (x-h)^2 + (y + a_i)^2 + \{\alpha[(z + d_k) - vt] + b_i\}^2$$

2.2. VECTORS OF THE ELECTROMAGNETIC FIELD

The strength components of the excited magnetic field and the induced electric field are determined as elements of the dual Maxwell's tensor $F_{ik}^{(\varepsilon)}$ [1, 2] (See Appendix 1). The dependencies

$$F_{ik}^{(\varepsilon)} = \frac{\partial \Psi_k}{\partial x_j} - \frac{\partial \Psi_j}{\partial x_k} \quad , (j,k = 1,2,3,4) \tag{11}$$

are used [1, 2 , 4].

For the magnetic field are obtained the following expressions

$$H_x = \frac{\alpha}{20\pi\mu} \sum_{i=1}^{5} \sum_{k=1}^{2} \left(\left[\frac{\Phi_k(t)(x+\delta)}{Q^{3/2}} - \frac{\Phi_k(t)(x-\delta)}{M^{3/2}} \right] \right) +$$

$$+ \frac{\varepsilon}{20\pi} \left\{ \sum_{i=1}^{5} \sum_{k=1}^{2} \frac{d^2\Phi_k(t)}{dt^2} \frac{\alpha[(z+d_k) - vt] + b_i}{P_i} \right\} \cdot \left(\frac{x+\delta}{Q_{ik}^{1/2}} - \frac{x+h}{C_{ik}^{1/2}} + \frac{x-l}{D_{ik}^{1/2}} - \frac{x-\delta}{M_{ik}^{1/2}} \right)$$

$$H_y = \frac{\alpha}{20\pi\mu} \sum_{i=1}^{5} \sum_{k=1}^{2} \left[\frac{\Phi_k(t)(y+a_i)}{Q_{ik}^{3/2}} - \frac{\Phi_k(t)(y+a_i)}{M_{ik}^{3/2}} \right] \tag{12}$$

$$H_z = \frac{\alpha}{20\pi\mu}\sum_{i=1}^{5}\sum_{k=1}^{2}\left[\frac{\Phi_k(t)\alpha[(z+d_k)-vt]+b}{Q_{ik}^{3/2}} - \frac{\Phi_k(t)\alpha[(z+d_k)-vt]+b}{M_{ik}^{3/2}}\right]+$$

$$+\frac{\alpha\varepsilon v^2}{20\pi\mu c^2}\left\{\sum_{i=1}^{5}\sum_{k=1}^{2}\Phi_k(t)\alpha[(z+d_k)-vt]+b_i\right\}.\left(\frac{1}{Q_{ik}^{3/2}}-\frac{1}{M_{ik}^{3/2}}\right)$$

and

$$E_x = \frac{\alpha v}{20\pi\mu c^2}\sum_{i=1}^{5}\sum_{k=1}^{2}\left[\frac{\Phi_k(t)}{\sqrt{Q_{ik}}}-\frac{\Phi_k(t)}{\sqrt{M_{ik}}}\right]$$

$$E_y = -\frac{\alpha v}{20\pi\mu c^2}\sum_{i=1}^{5}\sum_{k=1}^{2}\left[\frac{\Phi_k(t)(x+\delta)}{Q_{ik}^{3/2}}-\frac{\Phi_k(t)(x-\delta)}{M_{ik}^{3/2}}\right]-$$

$$-\frac{\alpha}{20\pi}\sum_{i=1}^{5}\sum_{k=1}^{2}\frac{d\Phi_k(t)}{dt}\frac{\alpha[(z+d_k)-vt]+b_i}{P_{ik}}\left[\frac{x+\delta}{Q_{ik}^{1/2}}-\frac{x-\delta}{M_{ik}^{1/2}}+\frac{x-l}{D_{ik}^{1/2}}-\frac{x+l}{C_{ik}^{1/2}}\right] \tag{13}$$

$$E_z = \frac{1}{20\pi}\sum_{i=1}^{5}\sum_{k=1}^{2}\frac{d\Phi_k(t)}{dt}\frac{(y+a_i)}{P_{ik}}\left[\frac{(x+\delta)}{\sqrt{Q_{ik}}}-\frac{(x-l)}{\sqrt{C_{ik}}}+\frac{(x-l)}{\sqrt{P_{ik}}}-\frac{(x-\delta)}{\sqrt{M_{ik}}}\right]$$

for the electric field strength.

2.3. NUMERICAL RESULTS

The calculations for the determination of the electric and magnetic field vectors for the linear induction system shown in Fig.1 are done using the following data : height of the inductor $h = 0.09\ m$, length of the inductor $L = 0.22\ m$, length of the magnetic pole $d = 0.04\ m$, width of the magnetic pole $c = 0.04\ m$, air gap $\delta = 0.01\ m$ and thickness of the conductive sheet $g = 0.002\ m$.

The distribution of the magnetic flux lines in the cross-section of the LIS is presented in Figure 3 .

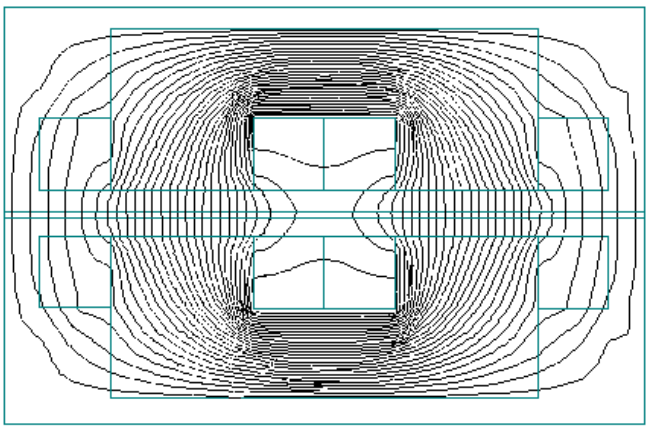

Figure 3. 2D flux lines for double polar LIS

The distribution curves of the magnetic field strength in the LIS are shown in Figure 4.

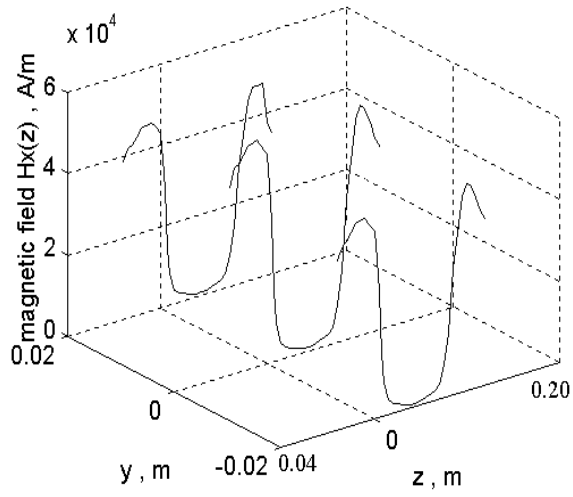

Figure 4 Distribution of the magnetic field in the air-gap
of the double-polar linear induction system

2.4. A COMPARATIVE ANALYSIS WITH FEM

The outline of the LIS analyzed with FEM is represented in Fig.5. The cross-section of the LIS is considered. In this case the vector-magnetic potential $\vec{A}_\mu$ is used in the analysis made by the FEM. The results are represented in Fig.6.

The distribution of the magnetic field strength in the air gap shows the same behaviour in the plane YOZ at $y=0$.

3. CONCLUSION

With the method represented in the paper one can determine the electromagnetic field components in the double-polar induction system using four-dimensional potential. A priority of this method is the obtaining of analytical results for the electromagnetic field components. The results obtained are valid for a linear system but they can be jointly used with the rest methods for analysis of linearized non-linear systems. The results are comparable to those got with the finite elements method for the investigated system .

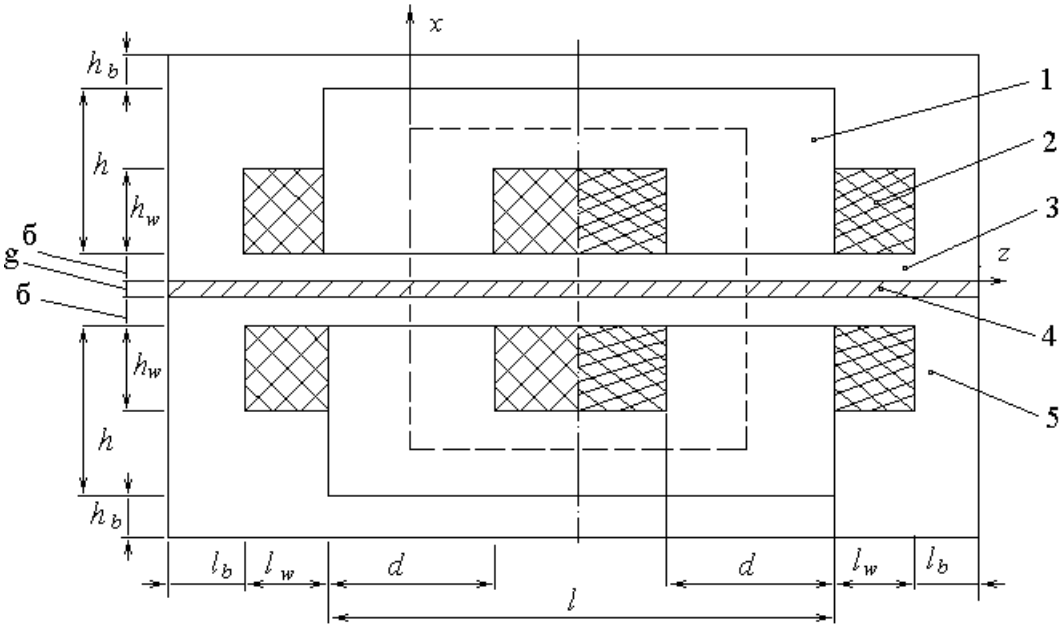

Figure 5. Outline of a double-pole LIS with two slots for FEM
Simulations:1-magnetic yoke; 2-exciting winding; 3- air ; 4-load metal shee ; 5- buffer area;
h – magnetic yoke height; h_w –tooth height; lw-slot length ; d – tooth width;
h_b-buffer height; l_b – buffer length; б –air gap; g – sheet thickness

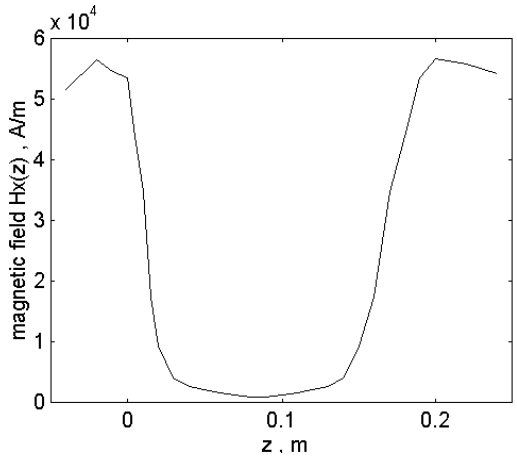

Figure 6. Distribution of the magnetic field in the air gap obtained by FEM

The investigations may be continued for determination of other characteristics, e.g. drag force, braking force, lift force etc., and as well as for an analysis of the electromagnetic field in multi-polar linear induction systems. Such systems at lower speeds of movement are the linear induction machines, liquid metal pumps, MHD generators etc., while at higher speeds – electromagnetic systems for magnetic resonance, electromagnetic guns, etc.

The method represented in this paper may be also used for optimization investigations as reported in [5] .

ACKNOWLEDGMENTS

The author is grateful to Prof. S.Papasov , Prof. N.Uzunoglu , Assos.Prof. G. Georgiev and A.Chervenkov for the informative critique , discussion and assembly of the manuscript .

APPENDIX 1

$$F_{ik} = \begin{bmatrix} 0 & -D_z & D_y & -\frac{j}{c}H_x \\ D_z & 0 & -D_x & -\frac{j}{c}H_y \\ -D_y & D_x & 0 & -\frac{j}{c}H_z \\ \frac{j}{c}H_x & \frac{j}{c}H_y & \frac{j}{c}H_z & 0 \end{bmatrix}$$

REFERENCES

[1] Chervenkova T.V. , Chervenkov A.G. ”Manifestation of the Differences Between Inductional Phenomena due to Movement and Variable Magnetic Flux “.ELECTROTECHNICA&ELECTRONICA , vol. XXIX No 7-8/1994. (in Bulgarian)

[2] Papazov S.P. , R.D. Stancheva. “ Electromagnetic effect exited by magnetic loops “, Archive fur Elektrotechnik 69(1986) 247-253.

[3] Stratton J.A. Electromagnetic theory. New York, London: McGraw-Hill 1941.

[4] Meerovich E.A., B.E. Meerovich. Methods of relativistic electrodynamics in engineering and electrophysic. Moscow 1987. (In Russian)

[5] Chervenkov A. “ A optimum shape of loop moving in magnetic field with non-sine structures ensuring maximum e.m.f. “ Second Symposium of Applied Electromagnetism of BSUAE, Xanth Greece , 27-29 June 2000.

[6] Dughiero F. , Lupi S. and Siega P. “ CALCULATION OF FORCES IN TRAVELING WAVE INDUCTION HEATING SYSTEMS “. IEEE Transactions on Magnetics, vol. 31, No 6, November 1995.